RSC Advances

PAPER

View Article Online
View Journal | View Issue

Cite this: *RSC Adv.*, 2016, **6**, 106201

Selective removal of BPA from aqueous solution using molecularly imprinted polymers based on magnetic graphene oxide

Rong-Zhong Wang,[ab] Dan-Lian Huang,*[ab] Yun-Guo Liu,*[ab] Zhi-Wei Peng,[ab] Guang-Ming Zeng,[ab] Cui Lai,[ab] Piao Xu,[ab] Chao Huang,[ab] Chen Zhang[ab] and Xiao-Min Gong[ab]

Received 23rd August 2016
Accepted 25th October 2016

DOI: 10.1039/c6ra21148h

www.rsc.org/advances

Bisphenol A (BPA) is a chemical with the potential to cause estrogenic and genotoxic effects on humans and wildlife. In this study, a novel and quick method was employed for selective removal of BPA from aqueous solutions, which used magnetic graphene oxide-based molecularly imprinted polymers as the adsorbent. Adsorption experiments were carried out to examine the effect of pH, initial concentration of BPA, isotherms and sorption kinetics on the adsorption of BPA by magnetic molecularly imprinted polymers (MMIPs). Results revealed the maximum adsorption capacity of BPA by MMIPs was 106.38 mg g^{-1} at 298 K and the equilibrium data of MMIPs were described well by a Langmuir isotherm model. Furthermore, the sorption kinetics followed the pseudo-second-order equation, which indicated that the chemical process might be the rate limiting step in the adsorption process for BPA. In addition, selective binding experiments were performed using 2,4-dichlorophenol and phenol as competitive compounds, and the resulting selectivity coefficients for the experiment were 2.505 and 2.440, respectively. All these results revealed that the prepared MMIPs had good selectivity and effective adsorption for BPA.

1. Introduction

Bisphenol A (2,2-bis(4-hydroxyphenyl)propane, BPA) is a chemical with the potential to cause estrogenic and genotoxic effects on humans and wildlife even at extremely low concentrations.[1–3] Over the past few decades, BPA has frequently been detected in drinking containers, consumer plastics, and environmental water.[4] Numerous methods have been used for the removal of BPA from the environment including adsorption,[5–7] ozonation,[8] membrane separation technology[9] and advanced oxidation processes.[10] However, it is highly resistant to chemical degradation, and biodegradable, conventional wastewater treatment methods are only partially efficient in removing it.[11] Additionally, these techniques cannot selectively remove BPA from complex matrixes, which limited their further application. For these reasons, searching for an appropriate adsorbent that has effective capacity and selective recognition is necessary.

Recently, molecularly imprinted polymers (MIPs), a type of tailor-made synthetic polymer with high affinity for target molecules, have gained worldwide attention.[12] MIPs are usually synthesized by polymerizing a crosslinking agent with a template–monomer complex. Following removal of the template, the specific binding sites which are complementary in size and shape to the template molecule are generated at the polymer.[13–15] Because of their predetermined selectivity, MIPs have been widely used in adsorption,[16] separation,[17] sensor devices,[18] catalysis[19] and so on.[20] However, the MIPs prepared by traditional methods suffer from some intrinsic limitations, such as poor site accessibility, time consuming, deeply buried binding sites in bulk and incomplete template removal.[21,22] With the purpose of overcoming the previously mentioned problems, the surface imprinting technique which designs the recognition sites on the surfaces of suitable substrates was employed.[23,24]

Graphene oxide (GO), with strictly two-dimensional materials and large specific surface area, has become an attractive carrier for preparing surface MIP composites.[25,26] Li *et al.* have developed a GO-based MIP platform for detecting endocrine disrupting chemicals.[26] The resulting composites exhibited high selectivity and outstanding affinity towards 2,4-dichlorophenol (2,4-DCP). Chen *et al.*[27] have reported an imprinted electrochemical sensor which is based on graphene for the determination of 4-nonylphenol. Mao *et al.*[28] have also successfully established an electrochemical sensor for dopamine using graphene sheets/Congo red MIP composites as a molecular recognition element. The prepared electrodes could determine dopamine with a wide linear range from 1.0×10^{7} to 8.3×10^{4} M. In addition, studies have reported that GO could

[a]*College of Environmental Science and Engineering, Hunan University, Changsha 410082, Hunan, People's Republic of China. E-mail: huangdanlian@hnu.edu.cn; liuyunguo@hnu.edu.cn; Fax: +86 731 88823987; Tel: +86 731 88822754*

[b]*Key Laboratory of Environmental Biology and Pollution Control (Hunan University), Ministry of Education, Changsha 410082, People's Republic of China*

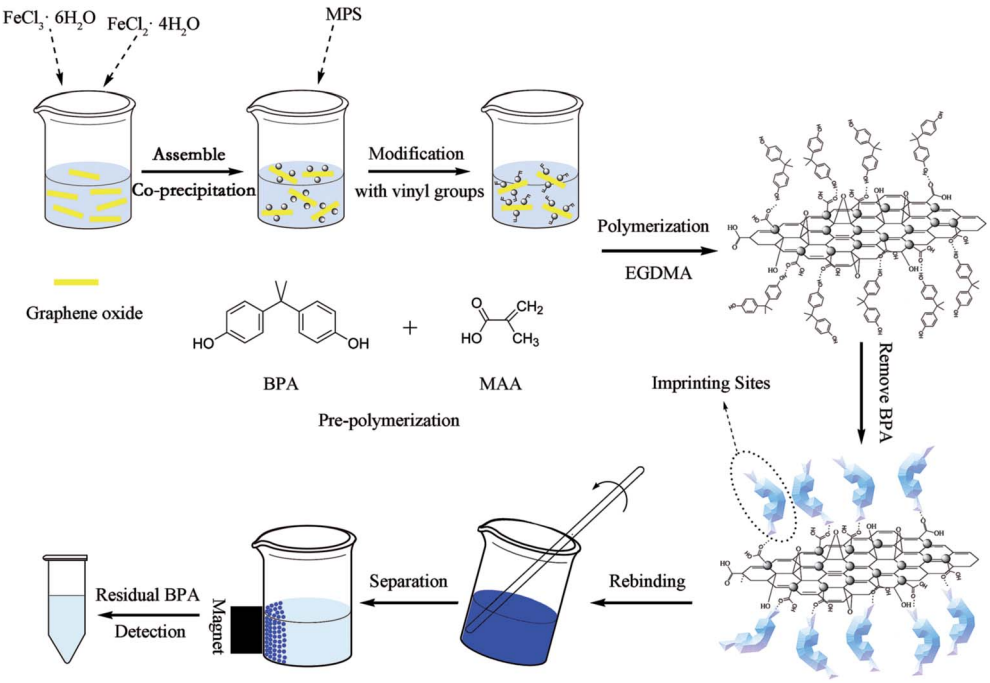

Fig. 1 Synthesis route of MMIPs and their application for the removal of BPA with the help of an applied magnetic field.

act as an adsorbent for BPA decontamination by π–π stacking interactions and hydrogen bonds.[29]

However, magnetite (Fe_3O_4) magnetic nanoparticles (MNPs) have caused considerable interest in catalysis, sensors and environmental remediation and this is attributed to their unique magnetic characteristics, eco-friendliness and biocompatibility in physiological environments.[30–32] Recently, the combination of magnetic particles and a surface imprinting technique have attracted more attention. By incorporating magnetic particles, the resulting magnetic molecularly imprinted polymers (MMIPs) can not only selectively recognize the target pollutant from complex samples, but can also be quickly collected and regenerated using an external magnetic field. The combination of the magnetic characteristic of MNP and the selectivity of MIP could widen the scope of their potential application.

In this research, a novel MMIP based on magnetic GO particles was successfully prepared for selective removal of BPA from aqueous solutions. The effect of pH, initial concentration of BPA, isotherms and sorption kinetics on the adsorption of BPA by the prepared MMIPs were examined in detail. Furthermore, the selectivity of the obtained MMIPs for BPA was evaluated in single and binary systems. The preparation route of MMIPs and their application for removal of BPA with the help of an external magnetic field is presented in Fig. 1.

2. Experimental

2.1. Materials and methods

BPA, tetrabromobisphenol A (TBBPA), phenol, 2,4-DCP, graphite powder, methacrylic acid (MAA), azobisisobutyronitrile (AIBN), oleic acid, ethylene glycol dimethylacrylate (EGDMA), dimethyl sulfoxide (DMSO), hydrogen peroxide (30% H_2O_2), poly(vinylpyrrolidone) (PVP), iron(II) chloride tetrahydrate ($FeCl_2 \cdot 4H_2O$) and ferric chloride hexahydrate ($FeCl_3 \cdot 6H_2O$) were purchased from Sinopharm Chemical Reagent Co., Ltd., (Shanghai, China). 3-(Methacryloyloxy)propyltrimethoxysilane (MPS) was purchased from Aladdin Industrial Corporation (Shanghai, China).

2.2. Preparation of MMIPs

GO was prepared from natural graphite powder using the modified Hummers' method.[33] Firstly, 35 mL of sulfuric acid, 0.6 g of graphite and 1.0 g of sodium nitrate were stirred together in an ice bath. After the graphite powder was well dispersed, 3 g of potassium permanganate was slowly added to the mixture and the temperature was kept below 10 °C. Subsequently, when the mixture was transferred to a 35 °C water bath and stirred for 30 min, 150 mL of deionized water (H_2O) was slowly added to the mixture with vigorous agitation. Then the mixture was stirred for about 15 min while the temperature was increased to 98 °C, followed by the slow addition of 200 mL of deionized water (60 °C). A portion (10 mL) of H_2O_2 (30%) was then added slowly into the previous mixture, which turned the color of the solution from dark brown to yellow. Finally, the resultant yellow-brown GO was washed with a 10% aqueous solution of hydrochloric acid and distilled water until the pH was 7.0 and then dried at 50 °C for 24 h.

Magnetic graphene oxide particles (MGO) were obtained *via* a co-precipitation technique.[34] GO (2.0 g) was dispersed into 180 mL of ultrapure water, which contained 4.72 g of $FeCl_3 \cdot 6H_2O$, with ultrasonic vibration for 30 min. In order to form a stable suspension, the mixture was stirred continually for 3.0 h. Subsequently, 1.72 g of $FeCl_2 \cdot 4H_2O$ was dissolved in the previous

mixture in a nitrogen (N_2) atmosphere and the solution heated to 80 °C. Then 10 mL of ammonium hydroxide solution (25%, w/w) was added dropwise to the solution with stirring, a black precipitate appeared immediately and the reaction was carried out for 30 min. Finally, the black precipitate was collected using an applied magnetic field. The materials obtained were dried under vacuum at 60 °C, and modified with MPS-introduced polymerizable double bonds. Simply, 0.45 g of MGO was dispersed in 75 mL of ethanol containing 5.0 mL of MPS, then the mixture was stirred at 40 °C for 12 h under continuous stirring. Finally, the products obtained were collected and washed with ethanol and water several times, and then dried under vacuum at 60 °C.

The MMIPs were synthesized according to a previous method reported in the literature with a few modifications, and the steps are listed next.[35] Firstly, 1.0 mmol of template (BPA) and 4.0 mmol of functional monomer (MAA) were dispersed into the 10 mL of DMSO. In order to obtain the pre-assembly solution, the mixture was stirred in an ultrasonic bath for 1.0 h. Subsequently, 1.0 g of MGO particles were blended with 2.0 mL of oleic acid and stirred for 10 min. Then, 20 mmol of EGDMA was added into the previous mixture and stirred continually for 30 min to obtain the pre-polymerization solution. Meanwhile, 0.4 g of PVP used as dispersant was dissolved in 120 mL of a solution of DMSO : H_2O (9 : 1, v/v) under stirring. Then, the pre-polymerization, pre-assembly solutions and 0.3 g of AIBN were added together into the solution of DMSO : H_2O. Then the mixture was purged with N_2 gas for 30 min and kept under 60 °C for 24 h. Upon completion, the polymers obtained were collected using a magnet, and then washed with a mixture of methanol/acetic acid (9 : 1, v/v) with Soxhlet extraction until no templates were detected in the rinses. Finally, the polymers obtained were dried at 60 °C for 24 h. As a reference, the magnetic non-imprinted polymers (MNIPs) were prepared using the identical synthetic protocol but omitting the BPA.

2.3. Adsorption experiments

Experimental parameters such as pH value (3–10), equilibration time (0–40 min), initial concentration of BPA (10–100 mg L^{-1}) were investigated in detail. In a study of the adsorption capacity, 0.01 g of sorbent (MMIPs or MNIPs) was dispersed into 50 mL of ethanol solution (25%, v/v) with various concentrations of BPA. The residual amount of BPA in the aqueous phase was measured using ultraviolet-visible spectrophotometry at 278 nm. The amount of BPA adsorbed on the MMIPs was calculated using the following eqn (1):

$$Q_t = (C_0 - C_t)V/W \quad (1)$$

where C_0 is the initial BPA concentration in solution (mg L^{-1}); C_t represents the residual concentration in solution at time, t (mg L^{-1}); V is the solution volume (L), and W is the mass of the adsorbent (g).

2.4. Binding selectivity

To measure the specificity of MMIPs, 0.01 g of the MMIPs were added into 100 mL flasks, each of which contained 50 mL of a solution of 500 mg L^{-1} of BPA, TBBPA, 2,4-DCP, or phenol. Furthermore, the competitive binding of MMIP for BPA were conducted by preparing mixtures of BPA and 2,4-DCP, and BPA and phenol. Sorbent (0.01 g; MMIPs or MNIPs) was added into a 100 mL flask, each of which contained 50 mL of a solution containing 500 mg L^{-1} BPA and interferences. The experiments were carried out on a shaker at 25 °C for 40 min. The static distribution coefficient (K_d), selectivity coefficients (k) and relative selectivity coefficients (k') were used to assess the selectivity of MMIPs. The previously mentioned parameters were calculated according to the following eqn (2)–(4):

$$K_d = Q_e/C_e \quad (2)$$

$$k = K_{d(BPA)}/K_{d(SC)} \quad (3)$$

$$k' = k_{MMIP}/k_{MNIP} \quad (4)$$

where Q_e and C_e are the adsorption capacity and equilibrium concentrations of BPA and similar compounds, respectively; $K_{d(BPA)}$ and $K_{d(SC)}$ are the static distribution coefficients of BPA and competitive compounds, respectively; k_{MMIP} and k_{MNIP} represent the selectivity coefficients of MMIPs and MNIPs, respectively.

3. Results and discussion

3.1. Characterization of adsorbents

The morphology of GO (a), MGO (b) and MMIPs (c) were examined using scanning electron microscopy (SEM), and the resulting patterns are shown in Fig. 2. In Fig. 2(a), GO displayed a relatively large surface area, and its morphology resembles a thin wrinkled curtain or crumpled flakes/sheet. As shown in Fig. 2(b), spherical and stick-like magnetic particles covered the surface of GO. Fig. 2(c) showed some agglomerates with a distribution of bead sizes. Generally, the type of reaction materials such as crosslinking monomer, initiator, and the reaction conditions such as reaction time, temperature and even the stirring speed could influence the morphology of the MMIPs to some degree.[35]

The Fourier-transform infrared (FT-IR) spectroscopy of the GO (curve a), MGO (curve b) and MMIPs (curve c) were measured and the results are shown in Fig. 3. The observed stretching vibration peak of 584.43 cm^{-1} (curve b and c) indicated that Fe_3O_4 was successfully embedded in the MMIPs. Furthermore, the MMIPs exhibited adsorption bands at around 1726.29 cm^{-1}, 1263.37 cm^{-1} and 1155.36 cm^{-1}, which were ascribed to the C=O stretching vibration, the C–O symmetric and asymmetric stretching vibration of the ester (EGDMA), respectively.[36] These results confirmed that the co-polymerization of MAA and EGDMA on the surface MGO in the presence of AIBN had been initiated. As can be seen from Fig. 4, which shows the X-ray diffraction (XRD) patterns, by comparing MMIPs with MGO, there were several relatively strong reflection peaks in the 2θ of 20–70°. The similar peak positions (220), (311), (400), (511) and (440) were at the diffraction angles of 30.23°, 35.37°, 43.23°, 57°, and 62.89°,[37]

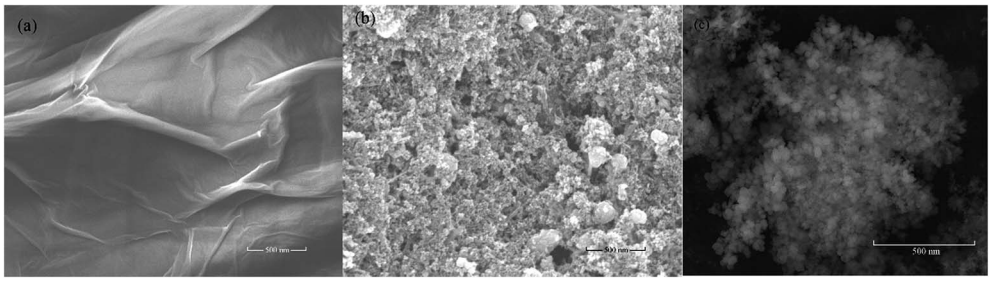

Fig. 2 SEM images of GO (a), MGO (b) and MMIPs (c).

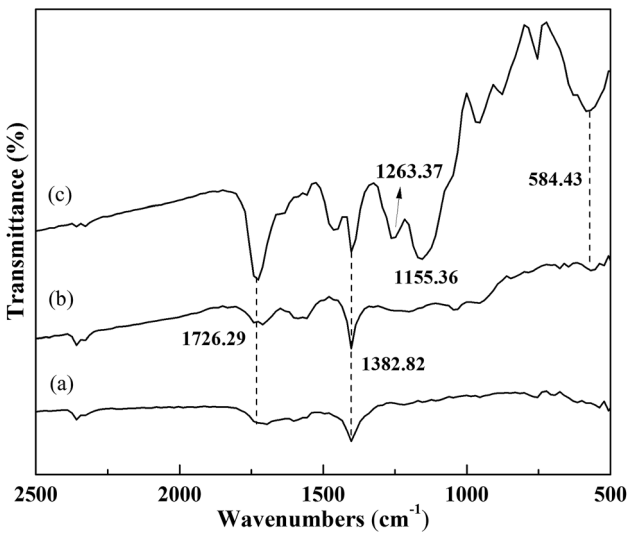

Fig. 3 FT-IR spectra and of GO (a), MGO (b) and MMIPs (c).

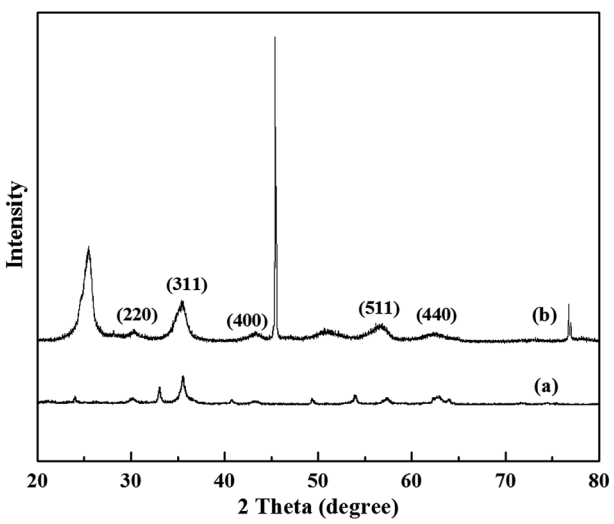

Fig. 4 X-ray diffraction (XRD) patterns of MGO (a) and MMIPs (b).

respectively. It was suggested that the MIP comprised Fe_3O_4 particles. The magnetic properties of Fe_3O_4 (a), MGO (b) and MMIPs (c) were characterized using vibrating sample magnetometry (VSM) and the results are shown in Fig. 5. Obviously, the M_s values of MMIPs was much lower than Fe_3O_4, because of the existence of non-magnetic MIP films. However, as shown in Fig. 5 (inset), the resulting MMIPs still possessed enough magnetic force that could be attracted by an external magnetic field.

The chemical composition of GO, MGO, MMIPs and MMIPs-1 (MMIPs after adsorbing BPA) was investigated using X-ray photoelectron spectroscopy (XPS). As can be seen from Fig. 6(a), the C 1s high resolution scan of GO, MGO, MMIPs and MMIPs-1 could be fitted into three peaks with binding energies of 284.8, 286.5 and 288.0 eV. The peak at ~284.8 eV was attributed to the C=C bonds in the polymer chain,[38] the peak at ~286.5 eV was attributed to C–O bonds[39] and the peak at 288 eV was explained by the presence of carbonyl groups.[40] The O 1s high resolution scan of GO, MGO, MMIPs and MMIPs-1 could be fitted into two peaks [Fig. 6(b)] with binding energies of 532 eV and 533 eV, which were attributed to an ester oxygen (O–C=O) and ether oxygen (C–O), respectively.[40] As can be seen from the results in Table 1, the decrease in the intensity of O 1s after adsorbing BPA may be associated with the entrapment of caffeine resulting in the swelling of the polymer.[40]

3.2. Adsorption study

3.2.1. Effect of contact time and kinetic study. The adsorption of BPA was studied kinetically and the results are presented in Fig. 7. The first initial adsorption of BPA by MMIPs was observed within 5 min, followed by a slow increase of the adsorbed amount until the adsorption equilibrium was reached. The adsorption rate was fast and the sorption amount of the MMIPs for BPA reached 293.28 mg g^{-1} in 5 min. After a quick adsorption, the kinetic curves for removal became stable at 40 min. The short contact time needed to reach equilibrium as well as the high adsorption capacity suggests that the MMIP possesses great potential application for the removal of BPA from aqueous solution. Compared with MMIPs, MNIPs also displayed some adsorption capacity for BPA, which may be attributed to the existence of GO. It is known that the surface of GO has different oxygen containing functional groups. These functional groups determine the charge, hydrophobicity, and electron density of the layers and alter the interaction between phenolic compounds and GO through π–π stacking interactions and hydrogen bonds.[29,41] Furthermore, some studies have reported that GO could act as an adsorbent for BPA decontamination. It was demonstrated that the π–π stacking interactions

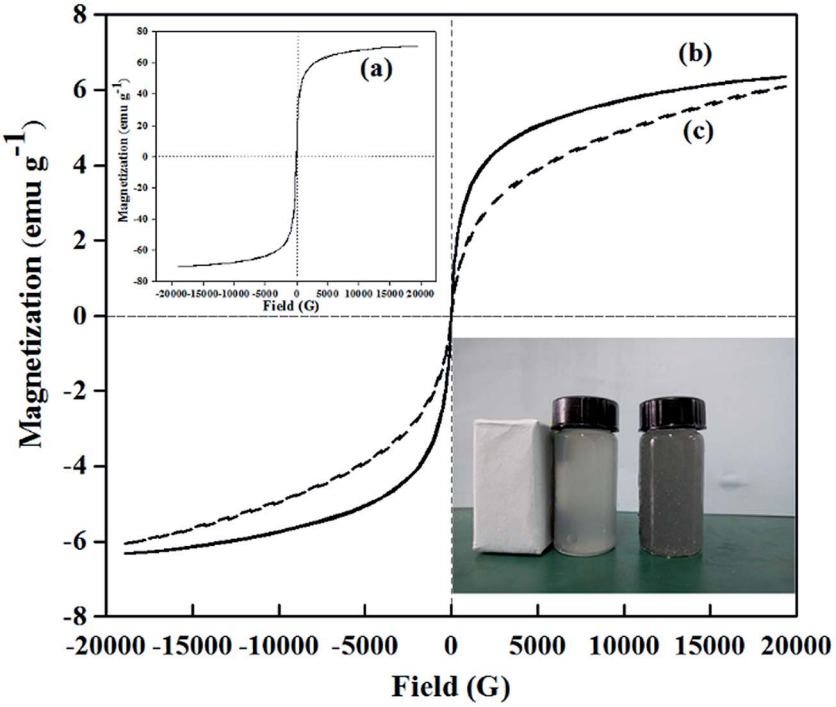

Fig. 5 VSM curves of Fe_3O_4 (a), MGO (b) and MMIPs (c). The inset shows the separation process of the solution of MMIP in the presence of an external magnetic field.

between six-membered carbon rings in GO and the aromatic rings in BPA were responsible for the adsorption process.[42] Furthermore, the MMIPs displayed a much higher binding capacity than those of MNIPs, which may be ascribed to the good formation of the specific sites on the surface of MMIPs.[43]

To further explore the underlying mechanisms of the adsorption of BPA using MMIPs and MNIPs, the pseudo-first-order equation and pseudo-second-order equation[44,45] models were applied to fit the experimental data. Two kinetic models can be expressed as eqn (5) and (6):

$$\ln(Q_e - Q_t) = \ln Q_e - k_1 t \quad (5)$$

$$t/Q_t = 1/k_2 Q_e^2 + t/Q_e = 1/h + t/Q_e \quad (6)$$

In eqn (5) and (6), Q_t (mg g^{-1}) represents the amount of BPA adsorbed at time t and Q_e (mg g^{-1}) at equilibrium, k_1 (min^{-1}) and k_2 (g mg^{-1} min^{-1}) are the rate constants of the pseudo-first order and the pseudo-second-order, respectively, and these can be calculated from the plot of $\ln(Q_e - Q_t)$ *versus* t and t/Q_t *versus* t, respectively. The value h represents the initial sorption rate (mg g^{-1} min^{-1}). All the rate constants of adsorption and linear regression values summarized in Table 2.

As can be seen from Table 2, the kinetic data was better fitted to pseudo-second-order equation than to pseudo-first-order equation, indicating that the chemical process may be the rate limiting step in the adsorption process for BPA, involving the hydrogen bond between the sorbent and the adsorbate.

3.2.2. Effect of initial pH. The initial pH of the solution plays a significant role in the adsorption process and it may affect the extent of the surface change of the adsorbent and the speciations of the pollutant.[46] Therefore, it was necessary to study the effect of pH on the adsorption. Fig. 8(a) shows the amount of BPA adsorbed by MMIPs or MNIPs at different pH values. It was observed that the highest amount that could be adsorbed was obtained when the pH was 6.0, which may be attributed to two types of adsorbent–adsorbate interactions. One main interaction was the binding affinity between targets and the specific imprinting sites.[34] The other was π–π interaction between the benzene rings of BPA and GO.[29] However, the adsorption capacity decreased significantly when the solution pH ranged from 6.0 to 10.0. This phenomenon may be associated with the pKa values of BPA and MAA, which were about 10.23 and 5.8, respectively.[47] When the pH is above 6, MAA, which was used in the synthesis of MMIPs has negative charge, the electrostatic repulsive interactions between BPA and MMIPs overcame the binding affinity and played an increasing role during the sorption process. Consequently, compared with the changes at acid conditions, the amount of BPA adsorbed dropped sharply when the value of the pH was above 6.0. Furthermore, the MMIPs had a higher adsorption capacity than the MNIPs throughout the entire pH-range investigated, strongly indicating a good imprinting effect.[35]

3.2.3. Effect of concentration and isotherm study. To estimate the binding properties of MMIPs for BPA, a saturation sorption experiment was used to measure the binding at various BPA concentrations. As can be seen from Fig. 9(a), the adsorbed amount of BPA by MMIPs increased with the increasing equilibrium concentration and finally reached saturation at a higher equilibrium concentration. Furthermore, the MMIPs exhibited a higher adsorption capacity than the MNIPs over the whole of

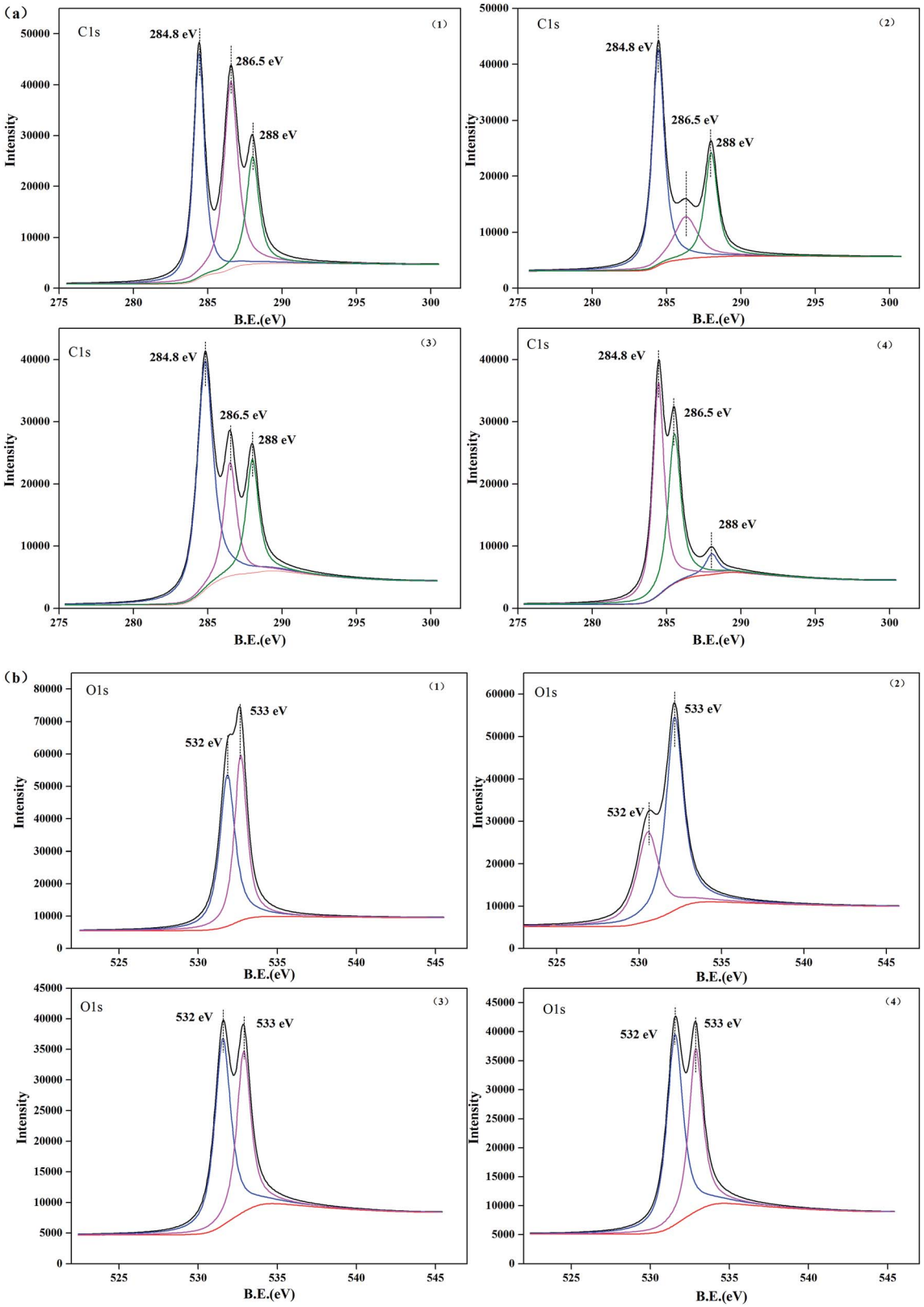

Fig. 6 XPS spectra of C1s (a) and O1s (b) for GO (1), MGO (2), MMIPs (3) and MMIPs after adsorption of BPA (4).

the concentration range. This was thought to probably be because of the molecular imprinting effect, which could selectively recognize the target pollutant *via* the specific binding formed in the MMIPs by the polymerization.[48] Because of the π–π interaction between the benzene rings of BPA and GO, MNIPs also displayed some adsorption capacity.[29]

Table 1 XPS quantification results for GO, MGO, MMIPs and MMIPs after adsorbing BPA (MMIPs-1)

Sample	Peak	Position BE (eV)	Atomic conc. (%)
GO	C 1s	296.62	60.061
	O 1s	541.52	37.719
MGO	C 1s	284.412	63.309
	O 1s	532.046	30.067
MMIPs	C 1s	296.52	67.731
	O 1s	541.42	25.809
MMIPs-1	C 1s	284.813	69.073
	O 1s	532.164	25.034

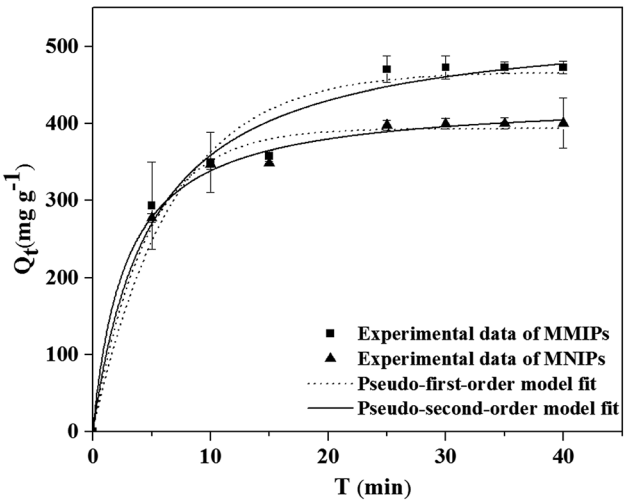

Fig. 7 Kinetic data and modeling for the adsorption of BPA onto MMIPs and MNIPs.

Table 2 Kinetic parameters of the pseudo-first-order and pseudo-second-order equations for adsorption of BPA on to MMIPs and MNIPs

Kinetics models	Constant	MMIPs	MNIPs
Pseudo-first-order	Q_e (mg g^{-1})	466.88	393.63
	k_1 (min^{-1})	0.1503	0.2237
	R^2	0.9597	0.9882
Pseudo-second-order	Q_e (mg g^{-1})	535.89	432.41
	K_2 (g mg^{-1} min^{-1})	0.0004	0.0008
	h (mg g min^{-1})	108.51	155.79
	R^2	0.9787	0.9961

The saturation binding data were further processed with the Freundlich and Langmuir equations to obtain the adsorption isotherms.[34,41] The equations can be expressed as follows:

$$Q_e = K_L Q_m C_e/(1 + K_L C_e) \quad (7)$$

$$Q_e = K_F C_e^{1/n} \quad (8)$$

where C_e is the equilibrium concentration of the adsorbate (mg L^{-1}); Q_e is the equilibrium sorption amount (mg g^{-1}); Q_m is the maximum sorption amount of the sorbate (mg g^{-1}); K_L is the affinity constant, where K_F (mg g^{-1}) is an indicative constant for adsorption capacity of the adsorbent and $1/n$, ranging between 0 and 1, measures the adsorption intensity or surface heterogeneity. The corresponding parameters of these models for adsorption of BPA are listed in Table 3.

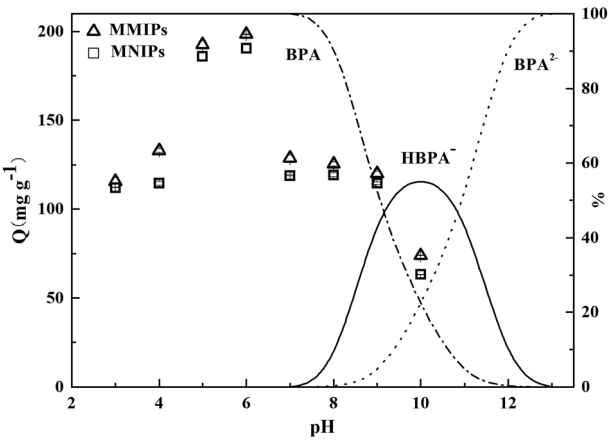

Fig. 8 Effect of initial pH on the BPA adsorption by MMIPs and MNIPs.

By fitting the experimental data with the Langmuir and Freundlich isotherm equations [Table 3 and Fig. 9(b)], it can be observed that the maximum adsorption capacity of BPA by MMIPs was 106.38 mg g^{-1} at 298 K and the equilibrium data of MMIPs were described well by the Langmuir isotherm model. Furthermore, MMIPs displayed a higher binding capacity for sorption of BPA than GO sorption.[49] The good fit obtained for the Langmuir model probably indicated that the chemical adsorption was dominant, which usually brings about monolayer adsorption on the surface of the MMIPs.

In addition, in order to further estimate the binding site heterogeneity of MMIPs, Scatchard analysis was conducted and the equation can be expressed as follows:

$$Q_e/C_e = (Q_{max} - Q_e)/K_{di} \quad (9)$$

where K_{di} (mg L^{-1}) is the dissociation constant of the binding sites; Q_{max} (mg g^{-1}) is the maximum amount of apparent binding; C_e (mg L^{-1}) is the equilibrium concentration of BPA; and Q_e is the equilibrium adsorption capacity. The Scatchard plot is shown in the inset of Fig. 9(a).

As can be seen from the inset of Fig. 9(a), the Scatchard plot for MMIPs was not a single linear curve, but consisted of two linear parts with different slopes. The linear equation for the left part of the curve of MMIPs was $Q_e/C_e = -0.189Q_e + 12.48$, and the K_{di} and Q_{max} were calculated to be 5.29 mg L^{-1} and 16.98 mg g^{-1}, respectively, for the polymer. The linear equation for the right part of the curve of MMIPs was $Q_e/C_e = -0.0509 + 5.7632$, and the K_{di} and Q_{max} were calculated to be 19.65 mg L^{-1} and 38.90 mg g^{-1}, respectively, for the polymer. It may be concluded that the binding site configuration in the MMIPs is heterogeneous in respect to the affinity for BPA.[50] Because of the π–π interaction between the benzene rings of BPA and GO, MMIPs displayed a certain amount of dsorption capacity in the whole process. The two linear relationships may indicate that

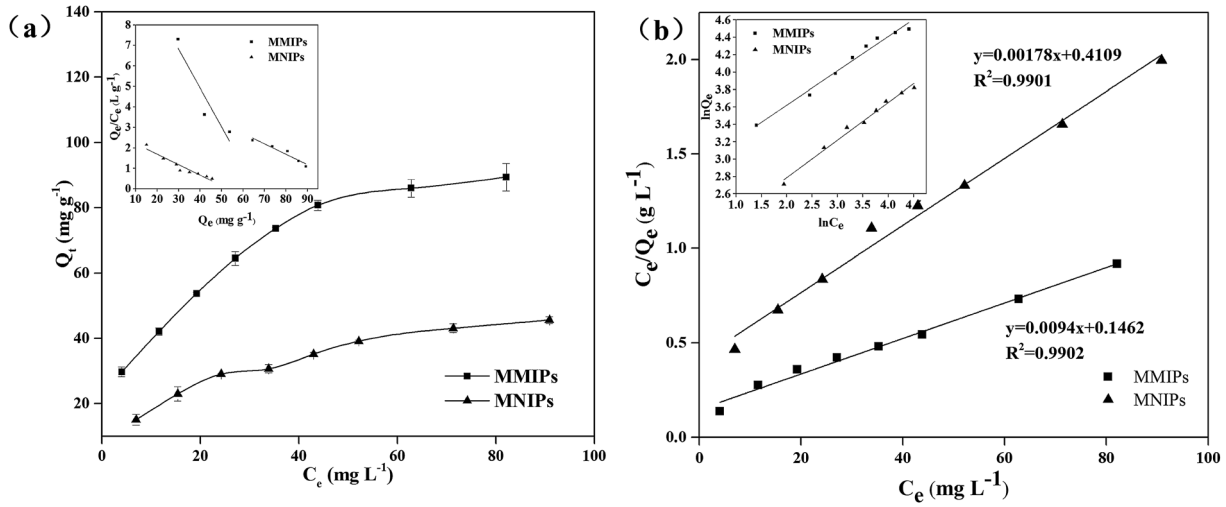

Fig. 9 Equilibrium data (a) and modeling for the adsorption of BPA onto MMIPs and MNIPs (b).

Table 3 Adsorption isotherm constants for MMIPs and MNIPs

Isotherm models	Constant	MMIPs	MNIPs
Langmuir	Q_m (mg g^{-1})	106.38	56.18
	k_L (L mg^{-1})	0.0026	0.0060
	R^2	0.9902	0.9901
Freundlich	n^{-1}	0.146	0.0066
	K_F (g mg^{-1})	6.84	15.13
	R^2	0.9816	0.987

two types of specific binding sites exist in MMIPs.[51] This is quite common for this kind of non-intervalence type MIP because different compounds were formed by the bonding between the imprinted molecule and the functional monomer.[37] Similar observations have been reported in the literature.[34] The binding of BPA to the MNIPs was also examined using the Scatchard method, and the Scatchard plot for MNIPs was a single straight line, which revealed that the binding sites of MNIPs were homogeneous.

3.3. Binding selectivity

3.3.1. Specific adsorption in a single pollutant system. In order to examine the specificity of MMIPs, the binding of MMIPs for BPA was compared to TBBPA, 2,4-DCP and phenol because they all had a certain degree of similar chemical structure, and the results are shown in Fig. 10. As illustrated in Fig. 10, MMIPs possessed the highest adsorption capacity for BPA out of the four adsorbates, and the adsorption capacity of MMIPs for the four compounds was much higher than that of MNIP. Because the specific sites which exist in the imprinted polymers are complementary in shape, size and spatial distribution to the template molecule, BPA has the advantage of occupying the binding sites over the other compounds.[34] However, because of the similar structural homology (–OH) to the template (BPA), the same hydrogen bond may form between the structural analog and functional monomers, thereby resulting in their adsorption capacity. Furthermore, there were no specific imprinted sites formed in the MNIPs, thus the MNIPs adsorbed the target contaminant by non-specific adsorption and showed low adsorption capacities.

3.3.2. Competitive adsorption in binary pollutant system. To further evaluate the selectivity of MMIPs for BPA, the batch experiments were conducted by preparing a mixture of BPA and 2,4-DCP, and a mixture of BPA and phenol, in which the initial concentration of each of the pollutants was 500 mg L^{-1}. Table 3 lists the results for relative selectivity coefficient, k', selectivity coefficient, k and the distribution coefficients, K_d. As shown in Table 4, MMIPs showed good selectivity for BPA in the mixture system. The values of k, suggest that the selectivity between the target pollutant and the other structural analogs were 1.770, and 2.403 for 2,4-DCP and phenol, respectively, indicating that the imprinting process was effective and MMIPs could selectively rebind BPA from complex samples. Furthermore, the relative selectivity coefficients k' for 2,4-DCP and phenol were 2.505 and 2.440, respectively, confirming that MMIPs had better

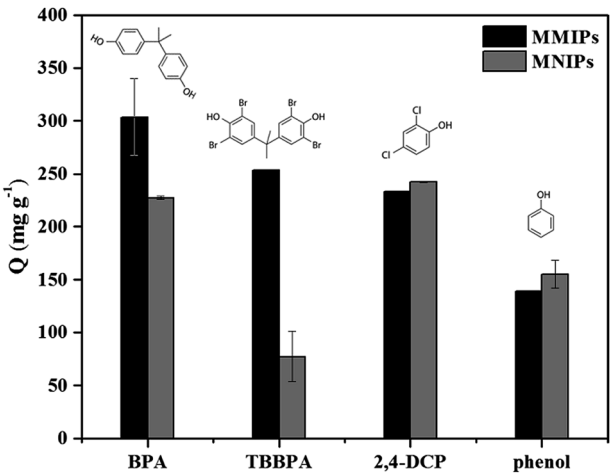

Fig. 10 The adsorption capacity of BPA, TBBPA, 2,4-DCP and phenol on MMIPs and MNIPs shown separately.

Table 4 Distribution coefficients (K_d), selectivity coefficients (k) of BPA in the mixture for MMIPs and MNIPs

Mixture		K_d (L g^{-1})		k		k'
		MMIPs	MNIPs	MMIPs	MNIPs	
BPA/2,4-DCP	BPA	1.282	0.207	1.770	0.707	2.505
	2,4-DCP	0.724	0.293			
BPA/phenol	BPA	2.055	1.726	2.403	0.985	2.440
	Phenol	0.855	1.752			

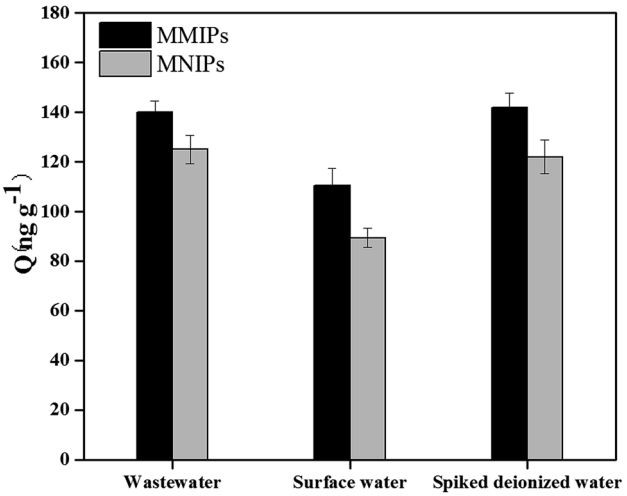

Fig. 11 Sorption of BPA from different water samples using MMIPs and MNIPs.

selectivity and sensitivity for BPA than MNIPs. From these results, it could be implied that the imprinted sites existing in MMIPs could distinguish BPA from its structural analogs.[34]

3.4 Removal of BPA from real water samples

In order to evaluate the feasibility of using MMIPs for removing BPA from complex matrices, surface water, spiked deionized water and a wastewater were applied to MMIPs. As can be seen from Fig. 11, MMIPs had a higher adsorption capacity than MNIPs. Also, the adsorption capacity of MMIP for BPA in deionized water was higher than in surface water and wastewater, suggesting that the capacity of MMIPs in removing BPA in real environmental water was reduced. This phenomenon may be attributed to the presence of many different organic/inorganic contaminants in environmental water bodies, which can also bind to MMIPs, thus reducing the adsorption capacity of MMIPs for BPA. The results suggested that there was a potential application for the MMIPs to be used to selectively remove BPA from water and wastewater.

4. Conclusions

In this work, a novel MMIP based on MGO particle was used as an effective and selective adsorbent for the removal of BPA from aqueous solution. Because of the imprinting effect and π–π stacking interactions between six-membered carbon rings in GO and aromatic rings in BPA, the composites prepared exhibited outstanding adsorption ability and fast mass transfer for BPA. The removal efficiency of BPA using MMIPs increased as the solution pH increased from 3.0 to 6.0. However, the adsorption capacity decreased significantly from pH 6.0 to 10.0. The results revealed that the maximum adsorption capacity of BPA on MMIPs was 106.38 mg g^{-1} at 298 K and the equilibrium data of MMIPs were described by a Langmuir isotherm model. Furthermore, the sorption kinetics followed the pseudo-second-order equation, which indicated that the chemical process may be the rate limiting step in the adsorption process for BPA. Furthermore, selective binding experiments revealed that MMIPs have a high adsorption capacity and selectivity towards BPA over other structurally related compounds. MMIPs provided a reliable and effective way to remove of BPA from aqueous water. Further studies should therefore focus on optimizing and testing the process under real conditions.

Acknowledgements

The study was financially supported by the Program for the National Natural Science Foundation of China (51378190, 51278176, 51408206, 51579098, 51521006), the National Program for Support of Top-Notch Young Professionals of China (2014), the Program for New Century Excellent Talents in University (NCET-13-0186), the Program for Changjiang Scholars and Innovative Research Team in University (IRT-13R17), Scientific Research Fund of Hunan Provincial Education Department (No. 521293050).

References

1 P. A. Hunt, K. E. Koehler, M. Susiarjo, C. A. Hodges, A. llagan, R. C. Voigt, S. Thomas, B. F. Thomas and T. J. Hassold, *Curr. Biol.*, 2003, **13**, 546–553.
2 M. V. Maffini, B. S. Rubin, C. Sonnenschein and A. M. Soto, *Mol. Cell. Endocrinol.*, 2006, **254**, 179–186.
3 I. D. S. Adamakis, E. Panteris and E. P. Eleftheriou, *Chemosphere*, 2016, **149**, 202–210.
4 A. V. Krishnan, P. Stathis, S. F. Permuth, L. Tokes and D. Fedman, *Endocrinology*, 2011, **132**, 2279–2286.
5 J. S. Mattson and H. B. Mark, *Activated carbon: surface chemistry and adsorption from solution*, Marcel Dekker, New York, 1971.
6 Y. Park, Z. Sun, G. A. Ayoko and R. L. Frost, *Chemosphere*, 2014, **107**, 249–256.
7 P. Xu, G. M. Zeng, D. L. Huang, C. L. Feng, S. Hu, M. H. Zhao, C. Lai, Z. Wei, C. Huang, G. X. Xie and Z. F. Liu, *Sci. Total Environ.*, 2012, **424**, 1–10.
8 M. Deborde, S. Rabouan, J. P. Duguet and B. Legube, *Environ. Sci. Technol.*, 2005, **39**, 6086–6092.
9 M. Gomez, G. Garralon, F. Plaza, R. Vilchez, E. Hontoria and M. A. Gómez, *Desalination*, 2007, **212**, 79–91.
10 E. J. Rosenfeldt and K. G. Linden, *Environ. Sci. Technol.*, 2004, **38**, 5476–5483.

11 J. H. Li, B. X. Zhou, Y. Q. Liu, Q. F. Yang and W. M. Cai, *J. Hazard. Mater.*, 2008, **151**, 389–393.
12 Y. Wu, Y. Liu, X. Gao, K. C. Gao, H. Xia, M. F. Luo, X. J. Wang, L. Ye, Y. Shi and B. Lu, *Chemosphere*, 2015, **119**, 515–523.
13 X. T. Shen, L. H. Zhu, N. Wang, L. Ye and H. Q. Tang, *Chem. Commun.*, 2012, **48**, 788–798.
14 N. Lavignac, C. J. Allender and K. R. Brain, *Anal. Chim. Acta*, 2004, **510**, 139–145.
15 R. C. Advincula, *Korean J. Chem. Eng.*, 2011, **28**, 1313–1321.
16 Y. Li, X. Li, Y. Q. Li, J. Y. Qi, J. Bian and Y. X. Yuan, *Environ. Pollut.*, 2009, **157**, 1879–1885.
17 H. S. Byun, Y. N. Youn, Y. H. Yun and S. D. Yoon, *Sep. Purif. Technol.*, 2010, **74**, 144–153.
18 M. Javanbakht, S. E. Fard, A. Mohammadi, M. Abdouss, M. R. Ganjali, P. Norouzi and L. Safaraliee, *Anal. Chim. Acta*, 2008, **612**, 65–74.
19 A. Strikovsky, J. Hradil and G. Wulff, *React. Funct. Polym.*, 2003, **54**, 49–61.
20 D. L. Huang, R. Z. Wang, Y. G. Liu, G. M. Zeng, C. Lai, P. Xiao, B. A. Lu, J. J. Xu, C. Wang and C. Huang, *Environ. Sci. Pollut. Res.*, 2015, **22**, 963–977.
21 D. M. Gao, Z. P. Zhang, M. H. Wu, C. G. Xie, G. J. Guan and D. P. Wang, *J. Am. Chem. Soc.*, 2007, **129**, 7859–7866.
22 B. J. Gao, J. Wang, F. Q. An and Q. Liu, *Polymer*, 2008, **49**, 1230–1238.
23 H. C. Chen, J. Kong, D. Y. Yuan and G. Q. Fu, *Biosens. Bioelectron.*, 2014, **53**, 5–11.
24 A. Mehdinia, T. B. Kayyal, A. Jabbari, M. O. A. Zanjani and E. Ziaei, *J. Chromatogr. A*, 2013, **1283**, 82–88.
25 H. M. Qiu, C. N. Luo, M. Sun, F. G. Lu, L. L. Fan and X. J. Li, *Anal. Chim. Acta*, 2012, **744**, 75–81.
26 Y. Li, X. Li, C. K. Dong, J. Y. Qing and X. Y. Han, *Carbon*, 2010, **48**, 3427–3433.
27 H. J. Chen, Z. H. Zhang, R. Cai, X. Chen, Y. N. Liu, W. Rao and S. Z. Yao, *Talanta*, 2013, **115**, 222–227.
28 Y. Mao, Y. Bao, S. Y. Gan, F. H. Li and N. Liu, *Biosens. Bioelectron.*, 2011, **28**, 291–297.
29 S. Bele, V. Samanidou and E. Deliyanni, *Chem. Eng. Res. Des.*, 2016, **109**, 573–585.
30 A. H. Lu, E. L. Salabas and F. Schüth, *Angew. Chem., Int. Ed.*, 2007, **46**, 1222–1244.
31 Y. Feng, J. L. Gong, G. M. Zeng, Q. Y. Niu, H. Y. Zhang, C. G. Niu, J. H. Deng and M. Yan, *Chem. Eng. J.*, 2010, **162**, 487–494.
32 J. L. Gong, B. Wang, G. M. Zeng, C. P. Yang, C. G. Niu, Q. Y. Niu, W. J. Zhou and Y. Liang, *J. Hazard. Mater.*, 2009, **164**, 1517–1522.
33 C. Wang, C. Feng, Y. J. Gao, X. M. Ma, Q. H. Wu and Z. Wang, *Chem. Eng. J.*, 2011, **173**, 92–97.
34 J. M. Pan, L. C. Xu, J. D. Dai, X. X. Li, H. Huang, P. W. Huo, C. X. Li and Y. S. Yan, *Chem. Eng. J.*, 2011, **174**, 68–75.
35 W. L. Guo, W. Hu, J. M. Pan, H. C. Zhou, W. Guan, X. Wang, J. D. Dai and L. C. Xu, *Chem. Eng. J.*, 2011, **171**, 603–611.
36 K. Yoshimatsu, K. Reimhult, A. Krozer, K. Mosbach, K. Sode and L. Ye, *Anal. Chim. Acta*, 2007, **584**, 112–121.
37 X. H. Gu, R. Xu, G. L. Yuan, H. Lu, B. R. Gu and H. P. Xie, *Anal. Chim. Acta*, 2010, **675**, 64–70.
38 Z. X. Jin, X. X. Wang, Y. B. Sun, Y. J. Ai and X. K. Wang, *Environ. Sci. Technol.*, 2015, **49**, 9168–9175.
39 J. B. Ma, H. W. Qiu, Q. H. Rui, Y. F. Liao, Y. M. Chen, J. Xu, P. P. Zhan and Y. G. Zhao, *J. Chromatogr. A*, 2016, **1429**, 86–96.
40 B. Schweiger, J. Kim, Y. J. Kim and M. Ulbricht, *Sensors*, 2015, **15**, 4870–4889.
41 T. Wu, X. Cai, S. Z. Tan, H. Y. Li, J. S. Liu and W. D. Yang, *Chem. Eng. J.*, 2011, **173**, 144–149.
42 J. Xu, L. Wang and Y. Zhu, *Langmuir*, 2012, **28**, 8418–8425.
43 F. J. Ning, H. L. Peng, J. H. Li, L. X. Chen and H. Xiong, *J. Agric. Food Chem.*, 2014, **62**, 7436–7443.
44 Y. S. Ho and G. McKay, *Water Res.*, 1999, **33**, 578–584.
45 Y. S. Ho and G. McKay, *Process Biochem.*, 1999, **34**, 451–465.
46 Q. Yu, S. B. Deng and G. Yu, *Water Res.*, 2008, **42**, 3089–3097.
47 B. K. Nandi, A. Goswami and M. K. Purkait, *J. Hazard. Mater.*, 2009, **161**, 387–395.
48 M. L. Noir, A. S. Lepeuple, B. Guieysse and B. Mattiasson, *Water Res.*, 2007, **41**, 2825–2831.
49 T. Phatthanakittiphong and G. T. Seo, *Nanomaterials*, 2016, **6**, 128.
50 C. M. Dai, J. Zhang, Y. L. Zhang, X. F. Zhou and S. G. Liu, *PLoS One*, 2013, **8**, e78167.
51 X. H. Gu, R. Xu, G. L. Yuan, H. Lu, B. R. Gu and H. P. Xie, *Anal. Chim. Acta*, 2010, **675**, 64–70.

